Minimal intestinal epithelial cell toxicity in response to short- and long-term food-relevant inorganic nanoparticle exposure

Christie McCracken,[†] Andrew Zane,[‡] Deborah A. Knight,[†] Prabir K. Dutta,[,‡] and W. James Waldman,*[,†]*

[†]Department of Pathology, The Ohio State University College of Medicine, Columbus, Ohio 43210, United States

[‡]Department of Chemistry and Biochemistry, The Ohio State University, Columbus, Ohio 43210, United States

*To whom correspondence should be addressed. Email: james.waldman@osumc.edu or dutta@chemistry.ohio-state.edu, Telephone: (614) 292-7772 or (614) 292-4532

Keywords: Silica, titania, zinc oxide, C2BBe1, cytotoxicity, nanoparticles, simulated digestion

Table of Contents Graphic

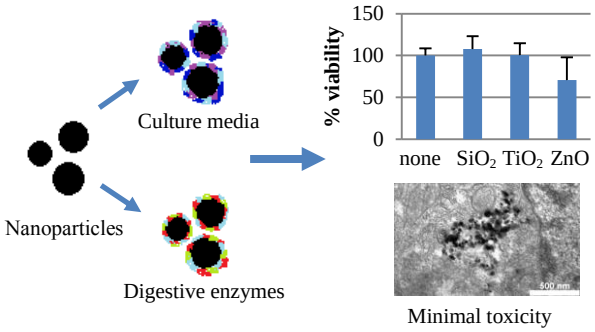

Abstract

Toxicity of commercial nanoparticles of titania, silica and zinc oxides is being investigated in this *in vitro* study. Particles of these compositions are found in many food items and thus this study is directed towards particle behavior in simulated digestion media and their interaction with intestinal epithelial cell line C2BBe1, a clone of Caco-2 cells, originally isolated from a human colon cancer. Even though the primary particle size of all three particles was below 50 nm, the particles appeared as aggregates in culture media with a negatively charged surface. In the presence of pepsin (~pH 2), the charge on the titania became positive, and silica was almost neutral and aggregated extensively, whereas ZnO dissolved. For silica and titania, treatment with simulated intestinal digestive solution led to a strongly negatively charged surface and particle sizes approaching values similar to those in media. Based on infrared spectroscopy, we concluded that the surface of silica and titania was covered with bile salts/proteins after this treatment. Transmission electron microscopy (TEM) indicated that the C2BBe1 cells internalized all three particles. Toxicity assays included investigation of necrosis, apoptosis, membrane damage and mitochondrial activity. Titania and SiO_2 particles suspended in media at loading levels of 10 $\mu g/cm^2$ exhibited no toxicity. With ZnO at the same loading level, mild toxicity was observed based only on the LDH assay and decrease of mitochondrial activity and not necrosis or apoptosis. Titania particles exposed to the simulated digestion media exhibited mild toxicity based on decrease of mitochondrial activity, likely due to transport of toxic bile salts via adsorption on the particle surface.

Introduction

The food industry has identified many potential applications for nanotechnology. Examples include nanoencapsulation to increase bioavailability of nutrients and provide controlled release, flavor enhancers, sensors using nanotechnology in food packaging and nanoparticles with antimicrobial properties.[1-3] Many of these applications are still being researched and may eventually find their way to the food products on the market. The Project on Emerging Nanotechnologies has compiled and periodically updates an inventory of consumer products containing nanoscale components, including products in the "Food and Beverage" category.[4] Despite the increased interest in using nanoparticles in food, the FDA currently has no specific regulations related to nanoparticles. A 2012 draft guidance suggested that food manufacturers investigate the safety of foods incorporating nanoparticles, but as of now, many of the inorganic nanoparticles are generally regarded as safe for use in foods.[5]

Silica (SiO_2) is used as an anti-caking agent and to clarify liquids, while titania (TiO_2) is commonly used as a whitening agent. The average size of food-grade TiO_2 (E171) and SiO_2 (E551) particles is a few hundred nanometers (nm), but both powders have broad size distributions. In an analysis of 89 consumer food products for TiO_2 content, 36% of E171 particles were found to have one dimension less than 100 nm.[6] Based on the TiO_2 detected in the tested food products, Weir et al.[6] estimated dietary exposure to TiO_2 for the US population to be 0.2-0.7 mg TiO_2/kg body weight/day for consumers over the age of 10 and 1-2 mg TiO_2/kg body weight/day for children under age 10 due to greater consumption of candies and sweets that tend to contain TiO_2. Food-grade SiO_2 was found to contain up to 33% silica with a size between 10-200 nm,[7] some of which would be considered nanoparticles according to the conventional definition of a nanoparticle as less than 100 nm. A study assessing the silica content of various foods estimated a "worst-case" intake of 1.8 mg/kg body weight/day nanosilica for the average adult (9.4 mg/kg body weight/day total silica).[7] These studies reveal that consumers are

currently being exposed to nano-sized fractions of both food-grade TiO_2 and SiO_2. However, individual exposure will vary greatly with diet.

As orally ingested nanoparticles traverse the digestive tract through the mouth, stomach, and intestines, they will be exposed to a number of digestive enzymes. The epithelial cells lining the small intestine absorb most nutrients obtained from food by endocytosis or diffusion and transport them across the epithelium where they can enter the bloodstream. As nanoparticles move through the small intestine, they will come into contact with intestinal epithelial cells, which may be able to internalize nanoparticles as they take up nutrients.

Previous *in vitro* and *in vivo* research has shown that nanoparticles do cross the intestinal epithelium, apparently by transcytosis, i.e. transport through the enterocytes.[8-10] Several studies have begun to investigate the toxicity of inorganic nanoparticles to intestinal epithelial cells both *in vitro*[9] and *in vivo*.[11-14] Based on the toxicity studies that have been conducted in different systems, it is apparent that toxicity depends upon many different properties of nanoparticles. Particle size influences toxicity, with nanoparticles showing greater toxicity than their larger counterparts.[15] Smaller particles have also been shown to be more readily internalized by intestinal epithelial cells.[8,10,15] Recently, nanoparticle characteristics other than size, including composition, solubility, crystal structure, surface charge, surface modifications, and shape have been recognized to substantially influence nanoparticle toxicity.[16-19]

In this paper, we investigated the internalization of commercially available nanoparticulate SiO_2, TiO_2, and ZnO, and examined their toxicity on C2BBe1 intestinal epithelial cells using several assays. To simulate the *in vivo* environment before interaction with the intestinal epithelium, nanoparticles were incubated with representative gastric and small intestinal digestive enzyme solutions before cell exposure. Long-term exposure during which cells were repeatedly treated with nanoparticles was also conducted. Data generated by these studies, the first to include long-term exposure in an *in vitro*

intestinal epithelial cell model, suggest that SiO_2 and TiO_2 exposed to culture media do not cause significant toxicity *in vitro* in their interactions with intestinal epithelial cells, whereas ZnO exhibits mild toxicity. However, TiO_2 treated with simulated digestion media do exhibit mild toxicity.

Experimental Procedures

Nanoparticles

Zinc oxide, titania, and silica nanoparticles were purchased from Sigma-Aldrich (St. Louis, MO). The specifications of the ZnO particles were size ≤ 100 nm, with a specific surface area of 15-25 m^2/g. For TiO_2, the particle size was specified as 21 nm, with surface area of 35-65 m^2/g, and purity of ≥ 99.5%, with a trade name of Aeroxide P25. Silica particle specification included size of 12 nm, with surface area of 175-225 m^2/g, and purity of 99.8%.

Particle Size and Surface Charge

A Zetasizer Nano ZS (Malvern, Westborough, MA) was used to determine the size and zeta potential of the particles. The Nano ZS uses a 633 nm laser as its light source. For size measurements, a 173° backscatter angle was used for collecting scattered light. The instrument was set to automatically determine the number of runs, the run duration, and the optimal focal point for each sample. The analysis model was set to general purpose, with default size limits of 0.4-10000 nm in diameter. Three replicate measurements were taken for all samples and averaged. All particle sizes are given as radii. For zeta potential measurements, a forward angle of 12° was used for collecting light. The default Smoluchowski model in the software program was used. Each measurement included 20 runs and monomodal analysis provided by the vendor was used for analysis. Three replicate measurements were taken for all samples and averaged. Samples were titrated versus pH using an attached MPT-2 Autotitrator. The titrator was supplied with 0.1 M HCl and 1.0 M HCl. Three replicate measurements were taken at each pH with a two minute pause between all measurements.

TEM Images of Commercial Nanoparticles

Images were taken using a Tecnai F20 Transmission Electron Microscope. Ten mg/mL solutions of each particle in ethanol were prepared and sonicated for 30 minutes. The solutions were dropped on to lacey carbon copper TEM grids (Ted Pella, Inc., Redding, CA) and allowed to dry for several hours.

Infrared Spectroscopy of Treated Particles

Diffuse reflectance infrared Fourier transform spectroscopy (DRIFTS) was performed on particles which had undergone simulated digestion treatment. After the final digestion step, the particles were washed twice with water. The digested particles were isolated by centrifugation and frozen with liquid nitrogen, then placed in a Millrock Bench Top Manifold Freeze Dryer (Millrock, Inc. Kingston, NY) to preserve any potential protein coating. The digestion protocol was performed on another set of particles using water in place of digestive enzymes to use as reference. DRIFTS analysis was performed with a Spectrum 400 FTIR Imaging System (Perkin Elmer, Waltham, MA). Scans were performed in percent reflectance mode, an air background (mirror in the diffuse reflectance cell) was collected, and then the water and digested samples (50 mg) were sequentially put into the cell (undiluted), and the spectrum recorded. Kubelka Munk analysis was done on these two samples using the air spectrum as background with a program developed in-house. The Kubleka-Munk spectrum obtained from the water-exposed sample was subtracted from the digested sample spectrum to analyze the coating on the particles (details of the subtraction procedure are provided in the Supplementary Section).

X-Ray Diffraction

X-Ray diffraction (XRD) analysis of the commercial particles was performed using a Rigaku Geigerflex diffractometer. Particles were packed onto glass slides with no further preparation. The diffraction angle was scanned from 0 to 100^{o} (2θ) with a 0.2 step size and 10 second dwell time.

Atomic Absorption Spectroscopy

Atomic absorption spectroscopy was performed to test for the presence of dissolved Zn ions after exposure of ZnO particles to the acidic pepsin enzyme solution. A Buck Scientific Accusys 211

spectrophotometer (East Norwalk, CT) was used with a Zn hollow cathode lamp (Heraeus). Standard solutions were diluted from 1000 ppm standard (Buck Scientific). The digestion protocol was performed on ZnO particles and stopped after exposure to pepsin solution. Following this, the solution was centrifuged at 209,000*g* for 30 minutes. The supernatant was removed and analyzed for Zn ion concentration.

Simulated gastrointestinal nanoparticle digestion

Pepsin, pancreatin, and bile salts were used to simulate the gastric and small intestinal digestive environments *in vitro*. The concentrations used were based on *in vitro* digestion methods used in previously published studies.[20-23] The stomach enzyme pepsin (146 U/mL, Sigma-Aldrich) was dissolved in water (pH 2, adjusted with 1N HCl). The small intestinal enzyme mixture pancreatin (2mg/mL, Sigma-Aldrich) was dissolved in water (adjusted to pH 7 with 1M $NaHCO_3$ and HCl). A solution of intestinal bile extract (porcine, Sigma-Aldrich) was made at a concentration of 0.024mg/mL in water (adjusted to pH 7 with 1M $NaHCO_3$ and HCl).

To simulate the digestive process, nanoparticles (50 mg/L) were incubated first in the pepsin solution for one hour (37^{o}C). The nanoparticles were pelleted by centrifugation (200,000 x g for 30 minutes) and resuspended in the pancreatin solution. After a one-hour digestion (37^{o}C), the particles were pelleted and resuspended in bile extract (one hour, 37°C). Nanoparticles were centrifuged and resuspended in phosphate-buffered saline (PBS) and used for the assays.

Cell Culture

C2BBe1 cells were obtained from the American Type Culture Collection (Manassas, VA) at passage 47 (as specified by the vendor). For short-term exposure assays, cells were used between passages 55-70, consistent with previous studies .[24-26]

Cells were cultured in Dulbecco's Modified Eagle Medium (DMEM; Life Technologies, Grand Island, NY) supplemented with 10% fetal bovine serum (FBS; Serum Source International, Inc.,

Charlotte, NC), 1 mM sodium pyruvate 2 mM L-glutamine, 0.3% penicillin/streptomycin, 0.3 ug/mL Amphotericin B (fungizone), and 10 μg/mL transferrin (all from Life Technologies). Cells were incubated in 10% CO_2/90% room air at 37°C. Cells were passaged every 5-7 days and plated on flasks or plates pre-coated with collagen I (0.05 mg/mL, rat tail, Life Technologies). Cells were incubated at least 24 hours prior to treatment with nanoparticles.

Treatment of cells with nanoparticles

The nanoparticles were weighed and placed in a glass vial prior to steam-sterilization. Sterile nanoparticles were suspended in PBS to make a 1 mg/mL solution. Immediately prior to treating cells, nanoparticle solutions were sonicated using a VC130 Sonics Vibra-Cell sonicator (Sonic Materials, Inc. Norwalk, CT) pulsing for one second on, one second off for approximately 15 seconds in order to break up nanoparticle agglomerates before exposing them to cells. Nanoparticles were added to cells at a dose of 10ug/cm^2 (100μL of the 1 mg/mL suspension per well of a 6-well plate in 2 mL total volume per well, or 20μL per well in a 24-well plate in 0.5 mL total volume per well). For assays described below, cells were seeded in 24-well tissue culture plates at a density of 2×10^4-1×10^5 cells/well and grown to 75-100% confluency. To promote contact of nanoparticles with cells, plates were centrifuged at 300×*g* for 15 minutes. Cells were incubated with nanoparticles for 24 hours at 37°C at 10% CO_2/90% air, and then washed twice with PBS. Toxicity assays were performed immediately after washing. For long-term nanoparticle exposure studies, culture media was added and cells were incubated at 37°C at 10% CO_2/90% air.

Long-term nanoparticle exposure studies

For long-term exposure studies, one exposure cycle consisted of plating cells in a 6-well tissue culture plate (Corning-Costar, Tewksbury, MA) pre-coated with collagen. After two days to allow the cells to firmly attach, cells were treated with 10μg/cm^2 nanoparticles and centrifuged to promote nanoparticle-cell contact. After a 24-hour incubation at 37°C, cells were washed with PBS and media was replaced.

Cells were cultured 4-6 days to reach confluency. Cells were then passed 1:10 into new 6-well plates and the nanoparticle treatment was repeated after each passage. This was continued for 29 nanoparticle exposure cycles. To perform toxicity assays, a portion of these long-term cultured cells were plated into 24-well tissue culture plates (Corning-Costar). Cells were treated with nanoparticles (10μg/cm^2) for 24 hours prior to each assay, as in single exposure studies. Long-term exposure studies were only conducted with commercially-obtained nanoparticles (i.e., no enzymatic digestion).

Cell growth

To assess the effects of long-term nanoparticle exposure on treated cells, we assessed their proliferation over a 10 day period. The cells were seeded at a density such that they reach confluence after 10 days. Cells were plated in triplicate into 6-well tissue culture plates at a density of 1×10^5 or 5×10^4 cells/well. The time at which cells were plated was considered time zero. Cells were counted daily using a Z2 Beckman Coulter Counter (Indianapolis, IN) and mean counts of triplicate wells were plotted versus time.

Sytox Red staining

To evaluate necrotic cell death (cellular membrane damage) in nanoparticle-treated cells, a flow cytometric analysis was performed using Sytox Red Dead Cell Stain (Life Technologies). Cells were treated with nanoparticles and briefly centrifuged. After a 24-hour incubation at 37°C, cells were washed twice with PBS and detached from the culture plate with trypsin. Each cell sample was suspended in 1 mL calcium- and magnesium-free Hanks Balanced Salt Solution (Life Technologies) and stained with 1 μL of the Sytox Red Dead Cell Stain. Samples were incubated for at least 15 minutes at room temperature before analyzing for fluorescence using a FACScalibur flow cytometer (BD Biosciences) at an excitation wavelength of 635 nm. All experimental conditions were performed in triplicate. As a positive control for cell death, a subset of wells were treated with 10 or 20 mM hydrogen

peroxide (H_2O_2) in DMEM for one hour. Culture medium was replaced and cells were incubated for 23 hours prior to staining and flow cytometric analysis.

Annexin V-FITC staining

To examine whether cells treated with nanoparticles underwent apoptosis, cells were stained with FITC-conjugated Annexin V (BD Biosciences, San Jose, CA). Cells were plated, treated with nanoparticles, and harvested with trypsin as described above. Cells were resuspended in 100 µL of Annexin binding buffer (Life Technologies). Five µL of FITC Annexin V was added to each tube and the samples were incubated for 15 minutes in the dark at room temperature before adding an additional 400 µL of Annexin binding buffer. Fluorescence of bound FITC Annexin V was then detected by flow cytometry, excitation wavelength of 488 nm. All experimental conditions were performed in triplicate. As a positive control for apoptosis, a subset of wells were treated with 10 or 20 mM H_2O_2 in DMEM for one hour. Culture medium was replaced and cells were incubated for 23 hours prior to flow cytometric staining and analysis.

LDH Assay

To further assess cell death by detecting cellular membrane damage, release of the cytosolic enzyme lactate dehydrogenase (LDH) into the culture medium was examined by colorimetric assay. Cells were plated and treated with nanoparticles as described above. After a 24-hour incubation, 50 µL of culture media was collected from each well and placed in a flat-bottom 96-well plate (BD Falcon). LDH activity was assessed using a commercially available kit (LDH Assay Kit, Sigma-Aldrich) according to manufacturer's instructions. Briefly, LDH Assay Substrate Solution, LDH Assay Cofactor Preparation, and LDH Assay Lysis Solution were added to samples and incubated at room temperature for 15-30 minutes. The absorbance was read on a microplate reader at 490 nm and 690 nm. Sample absorbance values were corrected by subtracting the background reading at 690 nm from the 490 nm reading. As a positive control for LDH release, cells were treated with a 1% solution of Triton X-100 (Sigma-Aldrich)

in DMEM for 5 minutes to lyse all cells before collecting the supernatants. Sample absorbance values were normalized to the Triton positive control (considered as 0% cell viability) and untreated negative control (considered as 100% cell viability). All experimental conditions were performed in quadruplicate.

MTT Assay

To measure the metabolic activity of nanoparticle-treated cells, we used a commercially available MTT assay kit (Cayman Chemical, Ann Arbor, MI). In this assay, the tetrazolium dye, MTT, is reduced by mitochondrial NAD(P)H-dependent oxidoreductase enzymes to an insoluble purple crystal, formazan. Cells were plated and treated with nanoparticles as described above and incubated for 24 hours at 37°C prior to the assay. As a positive control for complete cell death, cells were treated with a 1% solution of Triton X-100 in DMEM for five minutes immediately before the assay was performed. After the incubation, all but 150 µL of the cell media was removed from each culture well before the addition of 15 µL of the MTT reagent. The cells were incubated for 3-4 hours at 37°C. The culture media/MTT reagent was removed and formazan crystals were dissolved with the provided MTT solvent. The solution was transferred to a flat-bottom 96-well plate and absorbance values were read using a microplate reader at 570 nm and 690 nm. Absorbance values were corrected by subtracting the background absorbance reading at 690 nm from the absorbance at 570 nm. To analyze and compare the data, absorbance values were normalized to the untreated control cells such that the untreated control represented 100% mitochondrial activity and an absorbance of 0 represented the absence of mitochondrial activity (i.e., 0%). All experimental conditions were performed in quadruplicate.

TEM of nanoparticle-treated cells

To verify that treated cells internalized nanoparticles, TEM was performed. Cells were grown to near confluence in a 6-well tissue culture plate. Cells were then treated with nanoparticles and briefly centrifuged. After a 24-hour incubation at 37°C, the treated cells were washed twice with PBS before

detachment with trypsin. Detached cells were washed with PBS and resuspended in 3% glutaraldehyde in PBS. Incubation steps were carried out at room temperature on a Lab Line orbital shaker (Barnstead/Thermolyne, Melrose Park, IL) operating at 700 rpm. The cell suspension was centrifuged at 1000×*g* for 5 minutes between each processing step. Fixed cells were washed twice with sodium cacodylate buffer (pH 7.4, 10 minutes each), then post-fixed in 1% osmium tetroxide in sym-collidine buffer (pH 7.6) for 1 hour at room temperature. Following two washes with s-collidine buffer (10 minutes each) the cells were en-bloc stained with a saturated aqueous uranyl acetate solution (pH 3.3) for 1 hour. Cells were dehydrated in a graded ethanol series up to absolute (10 minutes each). Acetone was used as the transitional solvent for two 10-minute washes. Cells were infiltrated overnight with a 1:1 mixture of acetone and Spurr's epoxy resin (Electron Microscopy Sciences, Fort Washington, PA). Finally, the cells were centrifuged and the pellet was placed into BEEM™ embedding capsules containing 100% Spurr's resin. Polymerization of epoxy blocks was carried out at 70° C overnight. Polymerized blocks were sectioned with a Leica Ultracut UCT ultramicrotome (Leica Microsystem GmbH, Wein, Austria). Ultrathin (80 nm) sections were collected on 200 mesh copper grids (Electron Microscopy Sciences) and post-stained with lead citrate (3 minutes). Electron micrographs were generated on with a JEOL JEM-1400 TEM (JEOL Ltd. Tokyo, Japan) equipped with a Veleta digital camera (Olympus Soft Imaging Solutions GmbH, Műnster, Germany).

Results

Nanoparticle characteristics

The toxicity experiments were conducted with readily available commercial TiO_2, SiO_2, and ZnO nanoparticles. Particle specifications provided by the vendor appear above (*Experimental Procedures, Nanoparticles*) and results of characterization studies conducted in our laboratory are as follows. Figure 1A - C show the TEM pictures of the three particles; the primary particles of silica and titania are almost spherical with radii of ~ 10-15 nm for SiO_2, ~ 20 - 25 nm for TiO_2. For ZnO, there is a polydispersity in

size and morphology with both spherical (~10-20 nm) and rod-like (5-10×50-200 nm) particles. There is clearly some aggregation of these primary particles, and we discuss below the size based on dynamic light scattering which is used in this study rather than the primary size. Figure 2 shows the X-ray powder diffraction patterns, indicating that the SiO_2 is amorphous, TiO_2 is a mixture of anatase and rutile (marked on the figure, as is expected for P25), and ZnO is primarily wurtzite.

To simulate the digestion process that the particles would undergo in the gastrointestinal tract, particles were sequentially treated with pepsin at pH 2 to mimic the stomach, and then pancreatin and bile salts at pH 7 to mimic the small intestine. Particle characterization by light scattering and zeta potential measurements at each of these stages was measured and is summarized in Table 1. In the culture medium DMEM, all nanoparticles were negatively charged, with zeta potentials of -11 millivolt (mV) for TiO_2 and SiO_2, -19 mV for ZnO. The radii varied with ~96 nm for silica, ~112 nm for ZnO, and ~115 nm for titania. Titania particles remained stable in pepsin solution at approximately ~119 nm radii, but with a positive zeta potential of 14 mV. At the acidic pH (~ 2) of the pepsin solution, the surface of TiO_2 is protonated, consistent with the isoelectric point (IEP) of TiO_2 being pH ~ 6.[27] Silica particles had surface charge close to zero in the pepsin solution and aggregated to ~3000 nm particle radii, consistent with their IEP reported as pH 2,[28] and with our pH titration studies. ZnO particles dissolved during incubation in pepsin at pH 2. This is consistent with reports in literature[29,30] and was confirmed by measuring the dissolved Zn in the supernatant by atomic absorption spectroscopy, and the dissolved zinc correlated with the amount of nanoparticles introduced in the medium. Figure 3A is a plot of the size and zeta potential as a function of pH for ZnO in water and in the presence of media. In water, the ZnO particles are not tracked by light scattering below pH 6.5, indicating dissolution, whereas in the media there is a protective effect on the ZnO, and particle size only begins to decrease below pH 4. Dissolution studies were not done on the SiO_2 and TiO_2 particles, since these particles could be isolated after the various treatments and were used for the *in vitro* studies. Figure 3B shows the

difference infrared spectrum between ZnO that was exposed to media and that which was exposed to water (both samples lyophilized prior to infrared measurements, Supporting Information details the infrared procedure). Weak bands at 1661, 1534, 1444, 1395 cm^{-1} are characteristic of adsorbed protein, with the Amide 1 band at 1661 cm^{-1} suggesting the presence of β-sheet structures.[31] Similar bands were also noted for SiO_2 and TiO_2 exposed to media (not shown), indicating that protein adsorption is occurring on all particles exposed to media.

Upon treatment with pancreatin and bile salts, the zeta potentials of the TiO_2 and SiO_2 reversed and became strongly negative, in the range of -30 to -40 mV. TiO_2 particles retained their radii of ~ 104 nm, whereas SiO_2 deagglomerated and had radii of ~ 109 nm. Figure 4 shows the difference infrared spectra between the SiO_2 and TiO_2 that were exposed to pepsin, pancreatin and bile salts and those just exposed to water. The bands observed at 1682, 1527 and 1415 cm^{-1} are different from that observed with the media and stronger in intensity by about two orders of magnitude, indicating that the pepsin treatment alters the surface and promotes adsorption of material from the pancreatin/bile salt mix. Just based on the spectra, it is difficult to assign the exact types of species adsorbed on these particles. Infrared spectra reported in the literature on bile salts show presence of a band at 1680 cm^{-1},[32] and IR spectrum of just the bile salts used in this study show bands at 1625 and 1670 cm^{-1} (data not shown). These bands can be assigned to carboxylate groups of the bile salts, indicating that such species are adsorbed on the nanoparticle surface after treatment with the digestion medium.

Nanoparticle interaction with C2BBe1 cells

The intestinal epithelial cell line C2BBe1 was established as a sub-clone from Caco-2 cells, originally isolated from a human colon cancer,[33] to be a more homogeneous population of brush border-expressing cells.[34] These cells have been shown to form polarized monolayers of cells with microvilli maintained by cytoskeletal proteins, as is observed for intestinal epithelium *in vivo*.[35,36] For these studies, we used actively proliferating cells rather than differentiated cells since proliferating cells are generally more

sensitive to toxic agents as has previously been observed.[37] This level of sensitivity likely more accurately simulates the sensitivity of proliferating intestinal stem cells *in vivo*. As shown in Figure 5, morphology of C2BBe1 cells following exposure to TiO_2 (Figure 5B) is indistinguishable from that of untreated cells (Figure 5A).

In order to observe whether these nanoparticles are internalized by C2BBe1 cells, TEM was performed on cells that were treated with nanoparticles for 24 hours. Cells were treated with 10 $\mu g/cm^2$ of SiO_2, TiO_2, or ZnO and centrifuged. After 24 hours, cells were washed and processed for TEM. Each type of nanoparticle was able to be visualized within C2BBe1 cells, as shown in Figure 6, although there seemed to be differences in the amount of nanoparticle uptake as a function of the particle type. For all of the treated cells, nanoparticles were only found in a fraction of the cells. TiO_2 seemed to be taken up most readily by cells. All of the nanoparticles inside cells seemed to be clustered together, probably in vesicles. No particles were observed within the nucleus, only in the cell cytoplasm.

Toxicity

Cells were treated with nanoparticles at a dose of 10 $\mu g/cm^2$, centrifuged to promote nanoparticle-cell interaction, and incubated for 24 hours. Toxicity assays were then performed on the treated cells. Four different toxicity assays were performed. These short-term treatment experiments were conducted over a range of 5-12 cell passages (varying by assay).

Sytox Red is a nuclear stain that will bind DNA. However, it will only enter cells with damaged membranes and is thus a marker for cell necrosis or late apoptosis. Cells were stained with Sytox Red and analyzed by flow cytometry to measure the percent of stained cells (Figure 7A). Results are shown as percent viability based on normalization with unstained cells. The nanoparticle-treated cells showed comparable viabilities to the untreated control cells, approximately 100% viability, whereas H_2O_2 (used as a positive control) reduced viability of cells to 25%. Thus, SiO_2, TiO_2, and ZnO do not seem to cause necrotic cell death in C2BBe1 cells.

Flow cytometric analysis was also performed on cells stained with Annexin V to label apoptotic cells. Annexin V will bind to phosphatidylserine that is exposed on the outer surface of cells, which occurs in early apoptosis when phosphatidylserine is flipped to the outer layer of the cell membrane. C2BBe1 cells were stained with Annexin V and analyzed by flow cytometry (Figure 7B). Nanoparticle-treated cells revealed approximately 100% cell viability, which was similar to the untreated control cells. Inducing apoptosis with H_2O_2 as a positive control reduced cell viability to 10%. These results indicate that SiO_2, TiO_2, and ZnO do not induce apoptotic cell death in C2BBe1 cells.

The LDH assay indirectly measures cell death based on the amount of lactate dehydrogenase released by cells with damaged membranes. LDH release was measured in supernatants from C2BBe1 cells treated with nanoparticles for 24 hours and data were converted to percent viability of cells based on LDH release from positive control cells (treated with Triton X-100) and untreated control cells (Figure 7C). Both TiO_2 and SiO_2 showed comparable viability to the untreated control (near 100% viability) which supports the results of the flow cytometric assays. However, cells treated with ZnO displayed an approximately 20% ($p < 0.01$) decrease in viability from the control cells, indicating that ZnO is causing toxicity.

We also used the MTT assay to evaluate mitochondrial activity of these cells. The MTT assay measures the ability of cells to reduce a tetrazolium dye to the insoluble formazan, which can be measured colorimetrically. SiO_2 and TiO_2 particles induced no change in the mitochondrial activity, but ZnO treatment reduced mitochondrial activity to approximately 70% of untreated controls ($p < 0.0001$) (Figure 7D).

Toxicity of nanoparticles treated with digestive enzymes

C2BBe1 cells were also treated with SiO_2 and TiO_2 nanoparticles that had undergone simulated *in vitro* digestion. Since the ZnO dissolved in pepsin at pH 2, we could not treat cells with digested ZnO. Cells were treated with the digested nanoparticles, centrifuged, incubated for 24 hours, and toxicity

assays were performed as described above. Flow cytometric analysis after Sytox Red staining revealed no decrease in cell viability below that of the untreated control cells, suggesting no necrotic cell death induced by the digested nanoparticles (Figure 8A). Annexin V staining also revealed comparable cell viability between cells treated with digested nanoparticles and untreated control cells, suggesting that the digested nanoparticles do not induce cell apoptosis (Figure 8B). The digestion solutions appeared to interfere with the LDH assay (increase in apparent cell viability was observed after treatment of cells directly with only the digestive solutions; data not shown). Thus, LDH release could not be used as an indicator of digested nanoparticle toxicity. In the MTT assay, only the digested TiO_2 induced a slight decrease (10%) in mitochondrial activity (Figure 8C, $p < 0.02$), indicating that treatment with the digestion media caused minor nanoparticle toxicity.

Long-term C2BBe1 exposure to nanoparticles

Consumption of nanoparticles in foods can realistically be expected to result in repeated exposure of the intestinal epithelium to these particles over a protracted period. To examine the effects of long-term nanoparticle exposure on intestinal epithelial cells, C2BBe1 cells were treated with nanoparticles for 24 hours after each cell passage. Cells were plated and allowed to adhere and acclimate for 2 days before being treated with nanoparticles. After 24-hour treatment, free nanoparticles were removed and cells were grown to confluency. Cells were then passed into new plates and the particle exposure process was repeated. To examine the effects of repeated nanoparticle exposure on cells, some cells were also plated in 24-well plates for toxicity assays after certain cell passages. These cells were treated with nanoparticles for 24 hours before performing the toxicity assays described above.

Toxicity of nanoparticles on the long-term exposure cells (26 nanoparticle exposures) was determined using the same toxicity assays used for the acute exposure studies (Figure 9). Staining with Sytox Red and flow cytometric analysis revealed no changes in cell viability from the untreated control. Flow cytometric analysis of cells stained with Annexin V likewise showed no decrease in viability of the

cells. This suggests that the nanoparticles do not induce apoptosis in C2BBe1 cells even after repeated exposure. No decrease in viability was observed for cells treated with TiO_2 or SiO_2 by LDH assay. Measurement of LDH release from cells revealed a 30% decrease in viability in cells treated with ZnO ($p< 0.01$). A similar pattern was observed with ZnO treatment after all exposure cycles evaluated. This demonstrates that ZnO again may be inducing modest toxicity in cells exposed to ZnO long-term. No change in mitochondrial activity was observed after treatment with TiO_2 or SiO_2, however the MTT assay revealed a significant decrease of 55% ($p < 0.0001$) in mitochondrial activity in cells treated with ZnO.

Because long-term exposure to nanoparticles may induce effects other than cell death, growth curves were performed on long-term-exposed cells to measure changes in cell proliferation. Growth curves were conducted with cells repeatedly exposed to nanoparticles subsequent to the most recent nanoparticle treatment. Cell proliferation was measured by counting cells daily for 10 days, and growth curves were performed after 7, 11, 16, and 29 nanoparticle exposures. Figure 10 shows the growth curves obtained after 11 cycles.. The lack of differences among these growth curves suggests that long-term nanoparticle exposure did not affect cell proliferation. In Figure S2 (Supplementary Section), we show two replicate growth curves performed after 29 nanoparticle exposures. Although individual curves indicated slight differences between differentially treated cell populations, no reproducible trends were observed between the curves performed at any time points, and thus no further analysis was performed.

Discussion:

Particle Characteristics

From the X-ray diffraction patterns shown in Figure 2, silica is amorphous, ZnO has the wurtzite-type structure,[38] and TiO_2 is a mixture of anatase and rutile.[39]Table 1 shows that the size and charge of the particles undergo significant changes in different environments. In serum-containing media, the

particles appear aggregated as compared to the primary particle size (Figure 1), indicating that the as-obtained particles were aggregated, consistent with previous reports.[40,41] Titania becomes positively charged and the silica particles are almost neutral in the "stomach" fluid (pepsin, pH 2.0). In the case of silica, the neutrality of the particles results in formation of large aggregates (~ 3 μm radii). The charges revert back to negative in the neutral intestinal fluid and in the case of silica, the particles deagglomerate.

ZnO dissolved completely in the pepsin solution (pH 2.0). There are conflicting reports in the literature, with most studies suggesting that treatment at pH ~ 2 (simulating gastric conditions) will increase the solubility of ZnO, but at least one study suggests otherwise.[37] Light scattering studies as a function of pH shown in Figure 3A indicate that ZnO is indeed stabilized by the serum, and dissolution occurs at pH<4, as compared to ZnO in water, where rapid dissolution occurs at pH < 6.5. Infrared spectrum (Figure 3B) shows that upon suspension in serum, characteristic protein bands[31] are observed on the ZnO. It has been proposed that the presence of serum proteins will inhibit dissolution of ZnO,[40] however it is unlikely that serum can stabilize against dissolution in the highly acidic pepsin solution. Protein coronas are also observed on the TiO_2 and SiO_2 particles (Figure 4).

Particle Uptake by Cells

Our choice of a sub-clone (C2BBe1) of the Caco-2 cell line is based on their ability to mimic human intestinal cells. The Caco-2 cell line has been extensively characterized, and is recommended for use as an *in vitro* model of the GI tract by an international toxicity screening workgroup.[42] Figure 5 demonstrates that these cells form a confluent layer with intercellular tight junctions, the morphology of which is unaffected by nanoparticle exposure. The TEM data in Figure 6 indicate that particles are being internalized. Previous studies have also noted that silica with primary particle size of 32 and 83 nm were taken up by Caco-2 cells, formed larger agglomerates (200 - 300 nm), and even showed up in the nucleus after 72 hour exposure with the smaller particles.[43] Silica nanoparticle (NP) uptake by Caco-

2 cells by elemental analysis of the cells has been reported, although surface binding versus internalization is not readily distinguished by this method.[37] Internalization of TiO_2 NP in Caco-2 cells has also been reported.[9]

Toxicity: Undigested Particles

Engineered nanoparticles have been reported to interfere with optical assays due to light absorption/scattering effects.[44-46] In particular, for the MTT and LDH assays, it was suggested that loading levels be kept below 50 μg/cm^2. With ZnO at a loading level of ~ 10 μg/cm^2, slight effects were even observed with the LDH assay, but not with the MTT assay.[44] TiO_2 beyond loading levels of 100 μg/mL were found to adsorb on LDH.[45] SiO_2 has been reported to interfere with the MTT assay in HeLa cells by promoting exocytosis of the formazan crystals, even at loading levels of 10 μg/mL.[46] Because of these literature reports, the experiments in the present study were conducted at a dose of 10 μg/cm^2.

Silica/titania dispersed in cell media did not exhibit any toxicity by any of the assays, including the long-term study with repeated exposures (~ 29 cycles) (Figure 7,9). There is conflicting data in the literature on toxicity of silica. Lack of toxicity of SiO_2 in Caco-2 cells was observed despite particle internalization by cells and even nuclear localization of particles.[43] Mitochondrial activity (WST assay) in Caco-2 cells treated with SiO_2 NP showed no significant changes as compared to controls, even at dosage levels of 200 μg/mL.[43] In another study, SiO_2 NP were found to reduce cell viability only in undifferentiated Caco-2 cells, even at loadings of 5 μg/cm^2.[37]

With nanoparticles of TiO_2, there appears to be agreement of a lack of toxicity towards Caco-2 cells.[41] Commercial TiO_2 used in sunscreens, made up of a rutile core surrounded by $Al(OH)_3$ shell and fibrous-type morphology with lengths of 50 ±10 nm and widths of 7 ± 2 nm were not internalized, and no toxic effects were noted in response to loadings of up to 100 μg/mL.[47] TiO_2 at concentrations of 1-20 μg/cm^2 had no effect on Caco-2 cell viability in the presence or absence of serum.[40] TiO_2 at loadings of 0.1-100 mg/L did not influence Caco-2 cell viability, as measured by MTT assay.[41] TiO_2 at loading levels of 1-

10 μg/mL did not cause cell death, either after acute or chronic exposure in Caco-2 cells.[9] Anatase/rutile mixtures, similar to the NP examined in the present study, did not induce toxicity (by LDH assay) to Caco-2 cells at loading levels of 20 μg/cm^2, but toxicity was observed at 80 μg/cm^2. The WST-1 assay indicated reduction in metabolic activity only at loadings of 80 μg/cm^2.[48] Using the MTT assay, different mammalian cell types have been shown to respond differently to TiO_2 NP, with only some showing a toxic response.[49]

Zinc Oxide

In response to ZnO exposure, we found evidence of low-level cell toxicity as determined by the LDH assay, but this was not corroborated by assays of necrosis or apoptosis which demonstrated no toxicity (Figure 7C). Mitochondrial activity was also diminished by ZnO treatment (Figure 7D). Both these effects of ZnO were also observed in response to long-term treatment (Figure 9C,D). There is agreement in the literature that ZnO induces some cytotoxicity in Caco-2 cells.[41] ZnO have been reported to be cytotoxic to both undifferentiated and differentiated Caco-2 cells at doses > 5 μg/cm^2.[37]

Considering that TEM demonstrated that ZnO is internalized by cells, one hypothesis is that if the internalized ZnO NP are taken up in endosomes, the particles can dissolve and provide a burst of Zn^{2+} within the cell. The kinetic profile of pH change in Caco-2 endosomes upon internalization of particles indicates a drop in pH from 7.4 to ~ 5.[50] The intracellular dissolution hypothesis could explain the decreased mitochondrial activity observed in ZnO-treated cells. Zinc ions have been shown to be pro-apoptotic under certain circumstances[51] and the solubilized ZnO released from the endosomes could be causing toxicity by inhibiting energy metabolism.[51-53]

However, as Figure 10 shows, none of the three particles had any influence on the rate of proliferation of the cells.

Toxicity: Digested Particles

The MTT experiments suggest a slight decrease in metabolic activity induced by titania nanoparticles only after exposure to the simulated digestion solutions (Figure 8C). IR data shown in Figure 4 indicates that in both silica and titania, there is strong adsorption of material from the simulated digestive media. Bile salts/proteins appear to be on the surface of these particles, with the acidic pepsin treatment promoting the amount of adsorbed material (since particles exposed to media have much less material). Micelles of lecithin and the bile salt sodium deoxycholate at concentrations > 0.2 mM have also been reported to decrease cell viability of Caco-2 cells.[54] Thus, the nanoparticles could be transporting toxic material from the digestion media into the cells. It is unclear at this point why silica exposed to the simulated digestion media is not showing the same type of toxicity as the titania. It is important to note that the toxicity manifested by titania, as measured by the MTT assay, is mild and possibly can be related to the different levels of adsorbed bile salts being transported by the two particles.

Implications of this Study

The implications of this *in vitro* study of nanoparticles of SiO_2, TiO_2 and ZnO in media towards C2BBe1 cells are as follows. The cells internalized all three particles. ZnO were the only nanoparticles that induced mild toxicity by the LDH and MTT assay. Repeated exposure of cells to SiO_2, TiO_2 or ZnO did not alter their growth patterns or render them any more susceptible to toxicity. With the SiO_2 and TiO_2 treated with the simulated digestion medium, there was no indication of necrosis or apoptosis, but diminished mitochondrial activity was noted with titania, possibly due to transport of bile salts/proteins into the cell. The importance of the corona formed on nanoparticles is being recognized as important in toxicity,[55] since not only is the response of the living cell to the particle influenced by the composition of the corona layer, but it is also a mechanism to get material into the cells.

Even though we did not find SiO_2 and TiO_2 to be toxic, it is clear that they are internalized by the epithelial cells as nanoparticles and may subsequently enter the circulation and migrate to other parts of the body. The surface charge of SiO_2 and TiO_2 particles becomes neutral/positive within the

"stomach" solution and can therefore interact with the negative mucus proteins and influence their transport. With ZnO, toxicity is not relevant in its nanoparticulate form, unless stabilized against dissolution in the stomach. This is consistent with the observation that when ZnO was administered to rats by oral gavage, Zn^{2+} were found in tissues, but not as ZnO particles.[38] Thus, at least for silica and titania, it becomes essential to monitor transport of these nanoparticles *in vivo* to determine whether they do indeed enter the circulation and if so, to map their route(s) of distribution and potential sites of accumulation. Several studies have examined the fate of ingested nanoparticles. TiO_2 injected into rat ileum did not disrupt the structure of the epithelial layer, though the particles were taken up by the cells and eventually reached the liver.[14] *In vivo* studies with mice fed with SiO_2 exhibited liver toxicity.[56] Dynamics of the motion of nanoparticles into systemic circulation, localization in tissues and clearance from the body still needs to be mapped out.

Funding Sources

We acknowledge funding from USDA /NIFA (2011-67021-30360) for this research. PKD and WJW conceived this research and contributed equally to the work.

Supporting Information Available

The supporting information details the procedure for obtaining the infrared spectra as well as data on the growth curves after 29 nanoparticle exposures. This information is available free of charge via the Internet at http://pubs.acs.org/.

Abbreviations

Nanometer (nm)

Transmission electron microscopy (TEM)

Diffuse reflectance infrared Fourier transform spectroscopy (DRIFTS)

X-ray diffraction (XRD)

Phosphate-buffered saline (PBS)

Dulbecco's Modified Eagle Medium (DMEM)

Fetal bovine serum (FBS)

Lactate dehydrogenase (LDH)

Millivolt (mV)

Isoelectric point (IEP)

Nanoparticle (NP)

References

1. Sozer, N., and Kokini, J. (2009) Nanotechnology and its applications in the food sector. *Trends Biotechnol. 27*, 82-89.

2. Chaudhry, Q., and Groves, K. Nanotechnology Applications for Food Ingredients, Additives and Supplements. In *Nanotechnologies in Food*; Chaudhry, Q., Castle, L., and Watkins, R., Eds.; RSC Publishing: Cambridge, UK, 2010; pp 69-85.

3. Chaudhry, Q., Scotter, M., Blackburn, J., Ross, B., Boxall, A., Castle, L., Aitken, R., and Watkins, R. (2008) Applications and implications of nanotechnologies for the food sector. *Food Addit. Contam., Part A 25*, 241-258.

4. The Project on Emerging Nanotechnologies Consumer Products Inventory. http://www.nanotechproject.org/inventories/consumer/ (accessed June 20, 2013).

5. Draft Guidance for Industry: Assessing the Effects of Significant Manufacturing Process Changes, Including Emerging Technologies, on the Safety and Regulatory Status of Food Ingredients and Food Contact Substances, Including Food Ingredients that are Color Additives. http://www.fda.gov/Food/GuidanceRegulation/GuidanceDocumentsRegulatoryInformation/IngredientsAdditivesGRASPackaging/ucm300661.htm (accessed June 20, 2013).

6. Weir, A., Westerhoff, P., Fabricius, L., Hristovski, K., and von Goetz, N. (2012) Titanium dioxide nanoparticles in food and personal care products. *Environ. Sci. Technol. 46*, 2242-2250.

7. Dekkers, S., Krystek, P., Peters, R.J., Lankveld, D.P., Bokkers, B.G., van Hoeven-Arentzen, P.H., Bouwmeester, H., and Oomen, A.G. (2011) Presence and risks of nanosilica in food products. *Nanotoxicology 5*, 393-405.

8. Desai, M.P., Labhasetwar, V., Amidon, G.L., and Levy, R.J. (1996) Gastrointestinal uptake of biodegradable microparticles: effect of particle size. *Pharm. Res. 13*, 1838-1845.

9. Koeneman, B.A., Zhang, Y., Westerhoff, P., Chen, Y., Crittenden, J.C., and Capco, D.G. (2010) Toxicity and cellular responses of intestinal cells exposed to titanium dioxide. *Cell Biol. Toxicol. 26*, 225-238.

10. Jani, P., Halbert, G.W., Langridge, J., and Florence, A.T. (1990) Nanoparticle uptake by the rat gastrointestinal mucosa: quantitation and particle size dependency. *J. Pharm. Pharmacol. 42*, 821-826.

11. Wang, J., Zhou, G., Chen, C., Yu, H., Wang, T., Ma, Y., Jia, G., Gao, Y., Li, B., Sun, J., Li, Y., Jiao, F., Zhao, Y., and Chai, Z. (2007) Acute toxicity and biodistribution of different sized titanium dioxide particles in mice after oral administration. *Toxicol. Lett. 168*, 176-185.

12. Zhang, R., Niu, Y., Li, Y., Zhao, C., Song, B., Li, Y., and Zhou, Y. (2010) Acute toxicity study of the interaction between titanium dioxide nanoparticles and lead acetate in mice. *Environ. Toxicol. Pharm. 30*, 52-60.

13. Pasupuleti, S., Alapati, S., Ganapathy, S., Anumolu, G., Pully, N.R., and Prakhya, B.M. (2012) Toxicity of zinc oxide nanoparticles through oral route. *Toxicol. Ind. Health 28*, 675-686.

14. Onishchenko, G.E., Erokhina, M.V., Abramchuk, S.S., Shaitan, K.V., Raspopov, R.V., Smirnova, V.V., Vasilevskaya, L.S., Gmoshinski, I.V., Kirpichnikov, M.P., and Tutelyan, V.A. (2012) Effects of titanium dioxide nanoparticles on small intestinal mucosa in rats. *Bull. Exp. Biol. Med. 154*, 265-270.

15. Awaad, A., Nakamura, M., and Ishimura, K. (2012) Imaging of size-dependent uptake and identification of novel pathways in mouse Peyer's patches using fluorescent organosilica particles. *Nanomedicine 8*, 627-636.

16. Warheit, D.B., Webb, T.R., Reed, K.L., Frerichs, S., and Sayes, C.M. (2007) Pulmonary toxicity study in rats with three forms of ultrafine-TiO_2 particles: differential responses related to surface properties. *Toxicology 230*, 90-104.

17. Waldman, W.J., Kristovich, R., Knight, D.A., and Dutta, P.K. (2007) Inflammatory properties of iron-containing carbon nanoparticles. *Chem. Res. Toxicol. 20*, 1149-1154.

18. Nagy, A., Zane, A., Cole, S.L., Severance, M., Dutta, P.K., and Waldman, W.J. (2011) Contrast of the biological activity of negatively and positively charged microwave synthesized CdSe/ZnS quantum dots. *Chem. Res. Toxicol. 24*, 2176-2188.

19. Nagy, A., Harrison, A., Sabbani, S., Munson, R.S. Jr., Dutta, P.K., and Waldman, W.J. (2011) Silver nanoparticles embedded in zeolite membranes: release of silver ions and mechanism of antibacterial action. *Int. J. Nanomed. 6*, 1833-1852.

20. Mandalari, G., Faulks, R.M., Rich, G.T., Lo Turco, V., Picout, D.R., Lo Curto, R.B., Bisignano, G., Dugo, P., Dugo, G., Waldron, K.W., Ellis, P.R., and Wickham, M.S.J. (2008) Release of protein, lipid, and vitamin E from almond seeds during digestion. *J. Agric. Food Chem. 56*, 3409-3416.

21. Glahn, R.P., Wien, E.M., Van Campen, D.R., and Miller, D.D. (1996) Caco-2 cell iron uptake from meat and casein digests parallels in vivo studies: use of a novel in vitro method for rapid estimation of iron bioavailability. *J. Nutr. 126*, 332-339.

22. Reboul, E., Richelle, M., Perrot, E., Desmoulins-Malezet, C., Pirisi, V., and Borel, P. (2006) Bioaccessibility of carotenoids and vitamin E from their main dietary sources. *J. Agric. Food Chem. 54*, 8749-8755.

23. Connolly, M.L., Lovegrove, J.A., and Tuohy, K.M. (2010) *In vitro* evaluation of the microbiota modulation abilities of different sized whole oat grain flakes. *Anaerobe 16*, 483-488.

24. Amin, M.R., Orenuga, T., Tyagi, S., Dudeja, P.K., Ramaswamy, K., and Malakooti, J. (2011) Tumor necrosis factor-α represses the expression of NHE2 through NF-κB activation in intestinal epithelial cell model, C2BBe1. *Inflammatory Bowel Diseases 17*, 720-731.

25. Fredenburgh, L.E., Velandia, M.M., Ma, J., Olszak, T., Cernadas, M., Englert, J.A., Chung, S.W., Liu, X., Begay, C., Padera, R.F., Blumberg, R.S., Walsh, S.R., Baron, R.M., and Perrella, M.A.

(2011) Cyclooxygenase-2 deficiency leads to intestinal barrier dysfunction and increased mortality during polymicrobial sepsis. *J. Immunol. 187*, 5255-5267.

26. Bourgine, J., Billaut-Laden, I., Happillon, M., Lo-Guidice, J.M., Maunoury, V., Imbenotte, M., and Broly, F. (2012) Gene expression profiling of systems involved in the metabolism and the disposition of xenobiotics: comparison between human intestinal biopsy samples and colon cell lines. *Drug Metab. Dispos. 40*, 694-705.

27. Suttiponparnit, K., Jiang, J., Sahu, M., Suvachittanont, S., Charinpanitkul, T., and Biswas, P. (2011) Role of surface area, primary particle size, and crystal phase on titanium dioxide nanoparticle dispersion properties. *Nanoscale Res. Lett. 6*, 27.

28. Kosmulski, M., Hartikainen, J., Maczka, E., Janusz, W., and Rosenholm, J.B. (2002) Multiinstrument study of the electrophoretic mobility of fumed silica. *Anal. Chem. 74*, 253-256.

29. Mudunkotuwa, I.A., Rupasinghe, T., Wu, C-M., and Grassian, V.H. (2011) Dissolution of ZnO nanoparticles at circumneutral pH: a study of size effects in the presence and absence of citric acid. *Langmuir 28*, 396-403.

30. Bian, S-W., Mudunkotuwa, I.A., Rupasinghe, T., and Grassian, V.H. (2011) Aggregation and dissolution of 4 nm ZnO nanoparticles in aqueous environments: influence of pH, ionic strength, size, and adsorption of humic acid. *Langmuir 27*, 6059-6068.

31. Roach, P., Farrar, D., and Perry, C.C. (2006) Surface tailoring for controlled protein adsorption: effect of topography at the nanometer scale and chemistry. *JACS 128*, 3939-3945.

32. Kasthuri, J., and Rajendiran, N. (2009) Functionalization of silver and gold nanoparticles using amino acid conjugated bile salts with tunable longitudinal plasmon resonance. *Colloids Surf., B 73*, 387-393.

33. Fogh, J., Fogh, J.M., and Orfeo, T. (1977) One hundred and twenty-seven cultured human tumor cell lines producing tumors in nude mice. *J. Natl. Cancer Inst. 59*, 221-226.

34. Peterson, M.D., and Mooseker, M.S. (1992) Characterization of the enterocyte-like brush border cytoskeleton of the C2BBe clones of the human intestinal cell line, Caco-2. *J. Cell Sci. 102*, 581-600.

35. Peterson, M.D., and Mooseker, M.S. (1993) An in vitro model for the analysis of intestinal brush border assembly I. Ultrastructural analysis of cell contact-induced brush border assembly in Caco-2BBe cells. *J. Cell Sci. 105*, 445-460.

36. Peterson, M.D., Bement, W.M., and Mooseker, M.S. (1993) An in vitro model for the analysis of intestinal brush border assembly II. Changes in expression and localization of brush border proteins during cell contact-induced brush border assembly in Caco-2BBe cells. *J. Cell Sci. 105*, 461-472.

37. Gerloff, K., Pereira, D.I.A., Faria, N., Boots, A.W., Kolling, J., Förster, I., Albrecht, C., Powell, J.J., and Schins, R.P.F. (2013) Influence of simulated gastrointestinal conditions on particle-induced cytotoxicity and interleukin-8 regulation in differentiated and undifferentiated Caco-2 cells. *Nanotoxicology 7*, 353-366.

38. Baek, M., Chung, H-E., Yu, J., Lee, J-A., Kim, T-H., Oh, J-M., Lee, W-J., Paek, S-M., Lee, J.K., Jeong, J., Choy, J-H., and Choi, S-J. (2012) Pharmacokinetics, tissue distribution, and excretion of zinc oxide nanoparticles. *Int. J. Nanomed. 7*, 3081-3097.

39. Preda, S., Teodorescu, V.S., Musuc, A.M., Andronescu, C., and Zaharescu, M. (2013) Influence of the TiO_2 precursors on the thermal and structural stability of titanate-based nanotubes. *J. Mater. Res. 28*, 294-303.

40. De Angelis, I., Barone, F., Zijno, A., Bizzarri, L., Russo, M.T., Pozzi, R., Franchini, F., Giudetti, G., Uboldi, C., Ponti, J., Rossi, F., and De Berardis, B. (2012) Comparative study of ZnO and TiO_2 nanoparticles: physicochemical characterisation and toxicological effects on human colon carcinoma cells. *Nanotoxicology* [Online early access] DOI: 10.3109/17435390.2012.741724, published online Nov 9, 2012. http://informahealthcare.com/doi/full/10.3109/17435390.2012.741724 (accessed June 20, 2013).

41. Chalew, T.E.A., and Schwab, K.J. Toxicity of commercially available engineered nanoparticles to Caco-2 and SW480 human intestinal epithelial cells. (2013) *Cell Biol. Toxicol. 29*, 101-116.

42. Oberdörster, G., Maynard, A., Donaldson, K., Castranova, V., Fitzpatrick, J., Ausman, K., Carter, J., Karn, B., Kreyling, W., Lai, D., Olin, S., Monteiro-Riviere, N., Warheit, D., Yang, H., and ILSI Research Foundation/Risk Science Institute Nanomaterial Toxicity Screening Working Group. (2005) Principles for characterizing the potential human health effects from exposure to nanomaterials: elements of a screening strategy. *Part. Fibre Toxicol. 2*, 8.

43. Schübbe, S., Schumann, C., Cavelius, C., Koch, M., Müller, T., and Kraegeloh, A. (2012) Size-dependent localization and quantitative evaluation of the intracellular migration of silica nanoparticles in Caco-2 cells. *Chem. Mater. 24*, 914-923.

44. Kroll, A., Pillukat, M.H., Hahn, D., and Schnekenburger, J. (2012) Interference of engineered nanoparticles with in vitro toxicity assays. *Arch. Toxicol. 86*, 1123-1136.

45. Han, X., Gelein, R., Corson, N., Wade-Mercer, P., Jiang, J., Biswas, P., Finkelstein, J.N., Elder, A., and Oberdörster, G. (2011) Validation of an LDH assay for assessing nanoparticle toxicity. *Toxicology 287*, 99-104.

46. Fisichella, M., Dabboue, H., Bhattacharyya, S., Saboungi, M-L., Salvetat, J-P., Hevor, T., and Guerin, M. (2009) Mesoporous silica nanoparticles enhance MTT formazan exocytosis in HeLa cells and astrocytes. *Toxicol. In Vitro 23*, 697-703.

47. Fisichella, M., Berenguer, F., Steinmetz, G., Auffan, M., Rose, J., and Prat, O. (2012) Intestinal toxicity evaluation of TiO_2 degraded surface-treated nanoparticles: a combined physico-chemical and toxicogenomics approach in caco-2 cells. *Part. Fibre Toxicol. 9*, 18.

48. Gerloff, K., Fenoglio, I., Carella, E., Kolling, J., Albrecht, C., Boots, A.W., Förster, I., and Schins, R.P.F. (2012) Distinctive toxicity of TiO_2 rutile/anatase mixed phase nanoparticles on Caco-2 cells. *Chem. Res. Toxicol. 25*, 646-655.

49. Shukla, R.K., Sharma, V., Pandey, A.K., Singh, S., Sultana, S., and Dhawan, A. (2011) ROS-mediated genotoxicity induced by titanium dioxide nanoparticles in human epidermal cells. *Toxicol. In Vitro 25*, 231-241.

50. Blanchette, C.D., Woo, Y-H., Thomas, C., Shen, N., Sulchek, T.A., and Hiddessen, A.L. (2009) Decoupling internalization, acidification and phagosomal-endosomal/lysosomal fusion during phagocytosis of InlA coated beads in epithelial cells. *PLoS One 4*, e6056.

51. Plum, L.M., Rink, L., and Haase, H. (2010) The Essential Toxin: Impact of Zinc on Human Health. *Int. J. Environ. Res. Public Health 7*,1342-1365.

52. Brown, A.M., Kristal, B.S., Effron, M.S., Shestopalov, A.I., Ullucci, P.A., Sheu, K.F., Blass, J.P., and Cooper, A.J. (2000) Zn^{2+} inhibits alpha-ketoglutarate-stimulated mitochondrial respiration and the isolated alpha-ketoglutarate dehydrogenase complex. *J. Biol. Chem. 275*, 13441-13447.

53. Sheline, C.T., Behrens, M.M., and Choi, D.W. (2000) Zinc-induced cortical neuronal death: contribution of energy failure attributable to loss of NAD^+ and inhibition of glycolysis. *J. Neurosci. 20*, 3139-3146.

54. Tan, Y., Qi, J., Lu, Y., Hu, F., Yin, Z., and Wu, W. (2013) Lecithin in mixed micelles attenuates the cytotoxicity of bile salts in Caco-2 cells. *Toxicol. In Vitro 27*, 714-720.

55. Monopoli, M.P., Åberg, C., Salvati, A., and Dawson, K.A. (2012) Biomolecular coronas provide the biological identity of nanosized materials. *Nat. Nanotechnol. 7*, 779-786.

56. So, S.J., Jang I.S., and Han, C.S. (2008) Effect of micro/nano silica particle feeding for mice. *J. Nanosci. Nanotechnol. 8*, 5367-5371.

	SiO_2		TiO_2		ZnO	
	Size (r, nm)	Zeta Potential (mV)	Size (r, nm)	Zeta Potential (mV)	Size (r, nm)	Zeta Potential (mV)
DMEM/FBS	96 ± 4	-11 ± 0	115 ± 2	-11 ± 1	112 ± 2	-19.3 ± 1
Pepsin	3039 ± 321	+1 ± 2	119 ± 2	+14 ± 2	-	-
Pancreatin	109 ± 1	-38 ± 2	110 ± 0	-39 ± 2	-	-
Bile Salts	109 ± 4	-29 ± 2	104 ± 2	-35 ± 1	-	-

Table 1. Summary of dynamic light scattering data showing hydrodynamic radius and zeta potential of commercial nanoparticles during each step of a simulated digestion process.

A

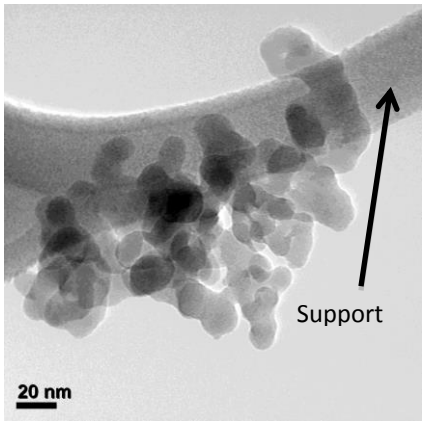

B

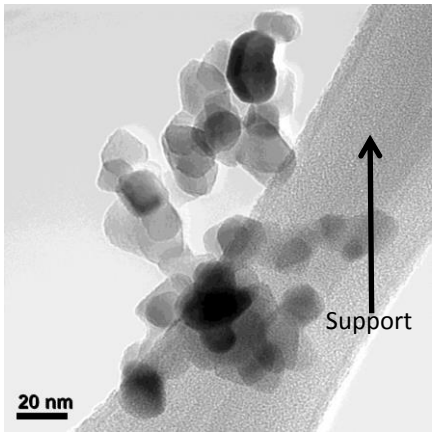

C

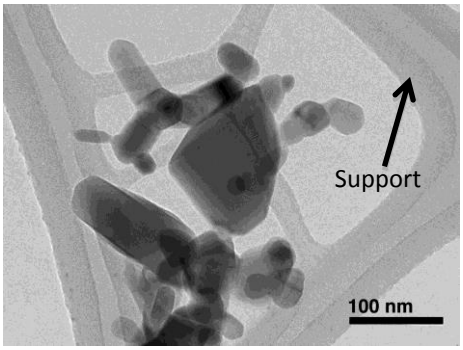

Figure 1. Representative TEM images of commercial nanoparticles. A) SiO_2, B) TiO_2, and C) ZnO. Long strands seen in the images are from the carbon support films, and indicated by arrows.

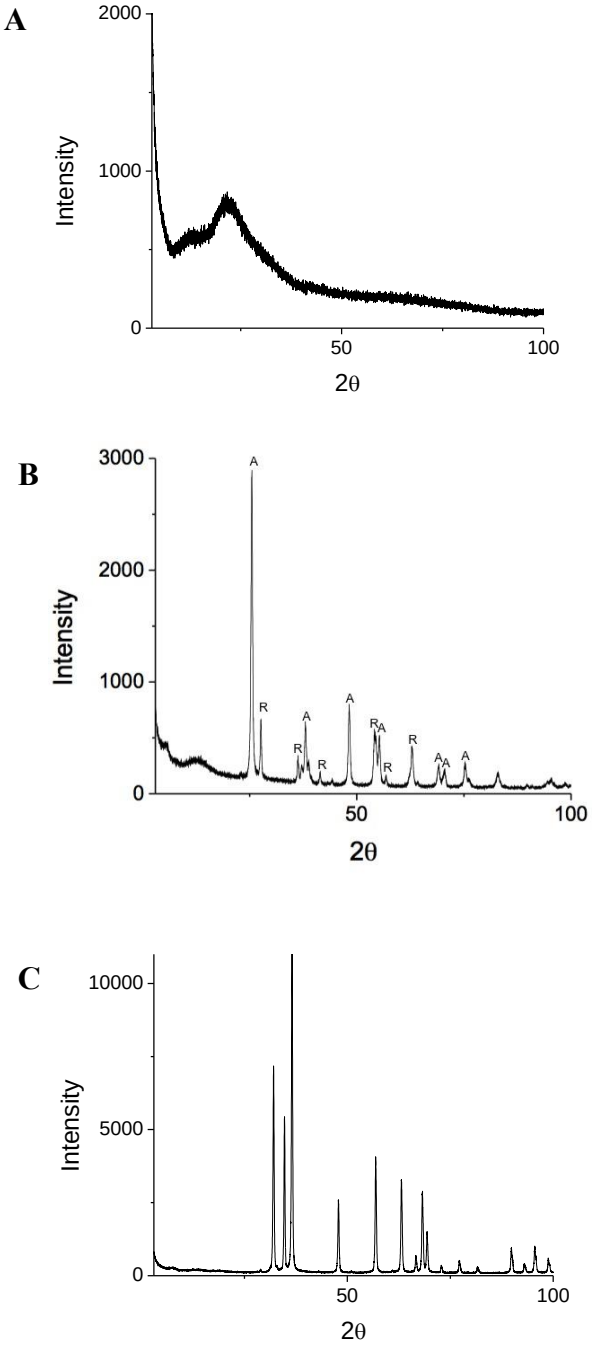

Figure 2. X-Ray Diffraction Patterns of commercial nanoparticles. A) SiO_2, B) TiO_2, (anatase and rutile peaks are marked by "A" and "R," respectively), and C) ZnO.

A

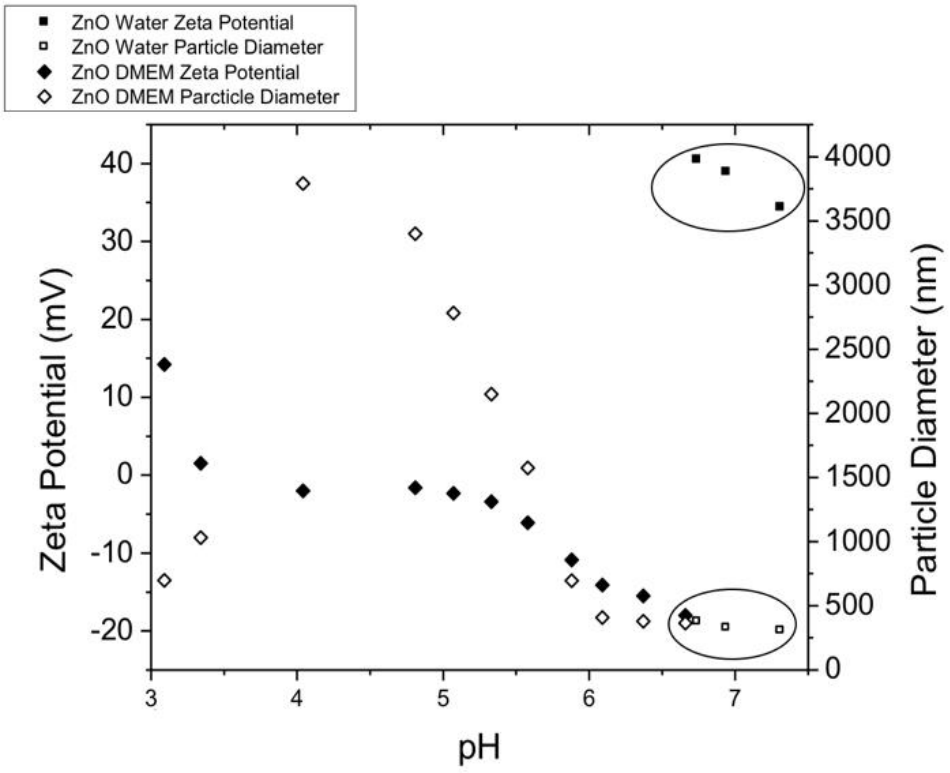

B

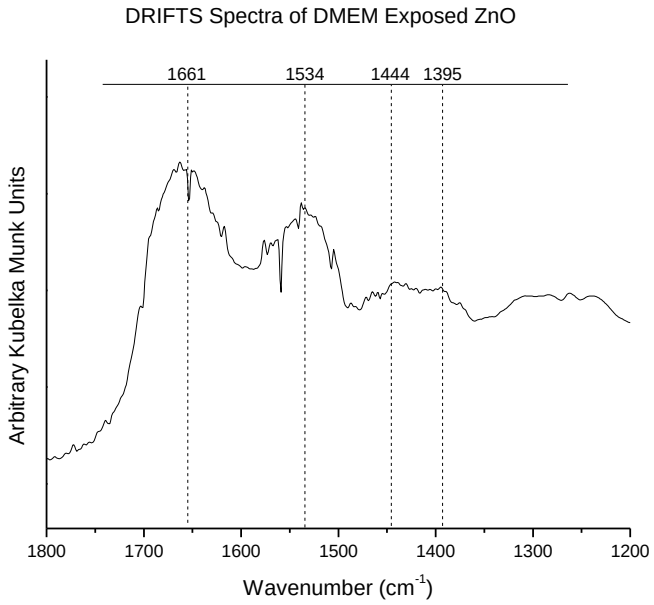

Figure 3. A) Particle size and zeta potential of ZnO during pH titration in media (diamond markers) and water (squares) (symbols used are on top left of figure). The water samples are circled for clarity. B) Difference infared spectrum in diffuse reflectance mode between ZnO particles exposed to DMEM/FBS media and water (y-axis in Kubelka-Munk arbitrary units). Supporting Information details the procedure used for the subtraction.

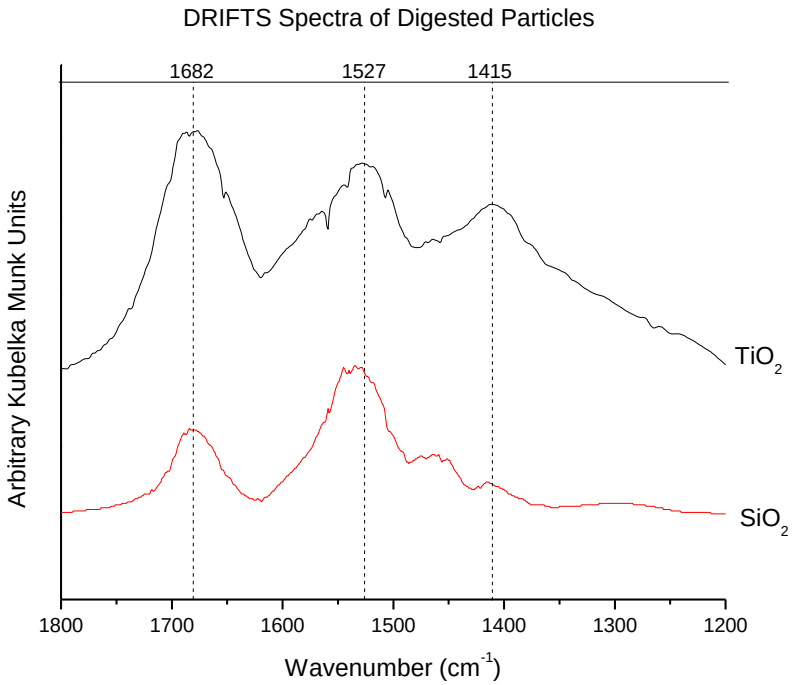

Figure 4. Difference infrared spectrum in diffuse reflectance mode between TiO_2 and SiO_2 nanoparticles treated with simulated digestion media and water (y-axis in Kubelka-Munk arbitrary units). Supporting Information details the procedure used for the subtraction.

A

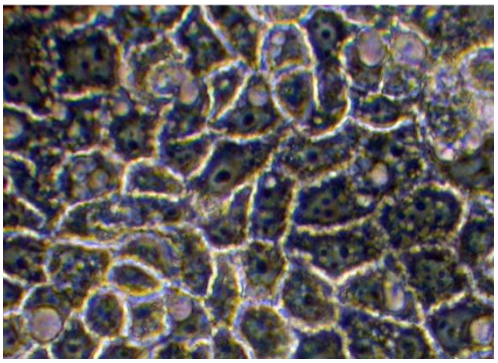

B

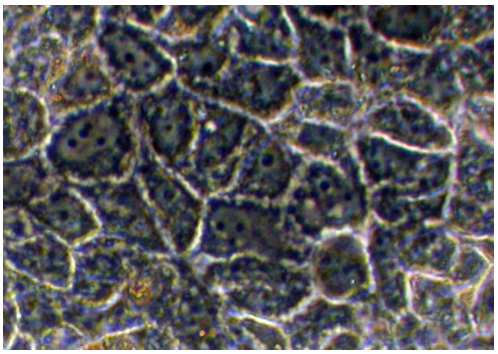

Figure 5. Cell morphology after nanoparticle treatment. A) Untreated control cells were compared to B) cells treated with TiO_2. Images were taken after TiO_2 was washed off cells.

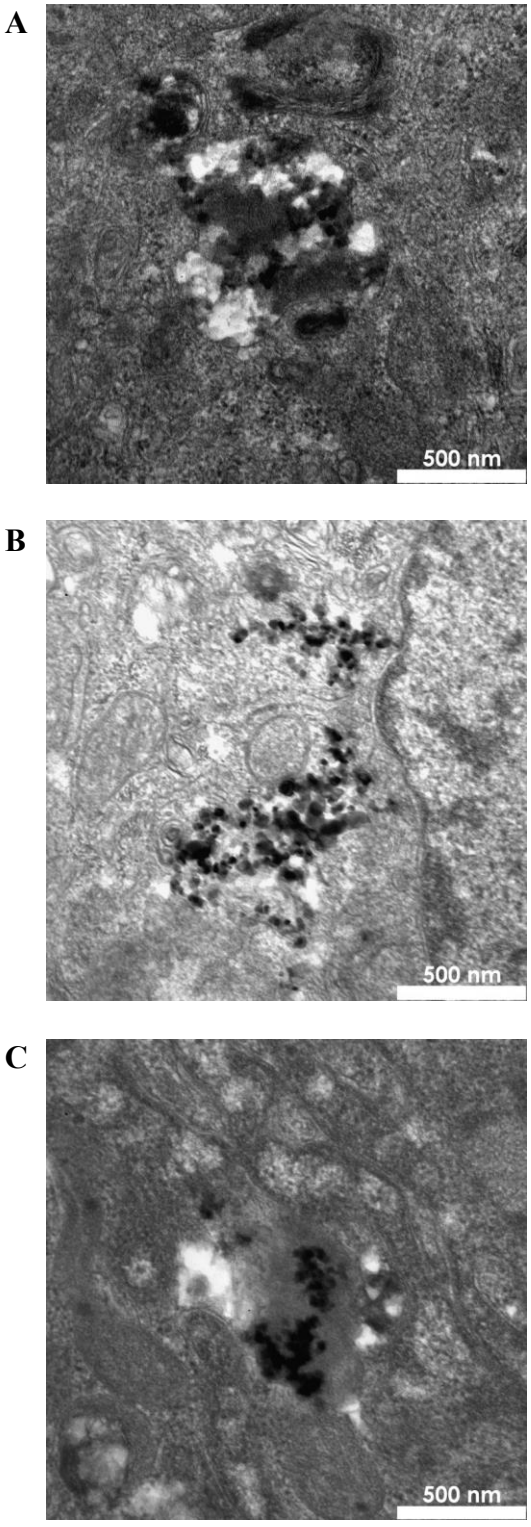

Figure 6. Representative TEM images of C2BBe1 cells which were treated with nanoparticles for 24 hours before being harvested, fixed in glutaraldehyde, and further processed for TEM. A) SiO_2-treated cell, B) TiO_2-treated cell, C) ZnO-treated cell.

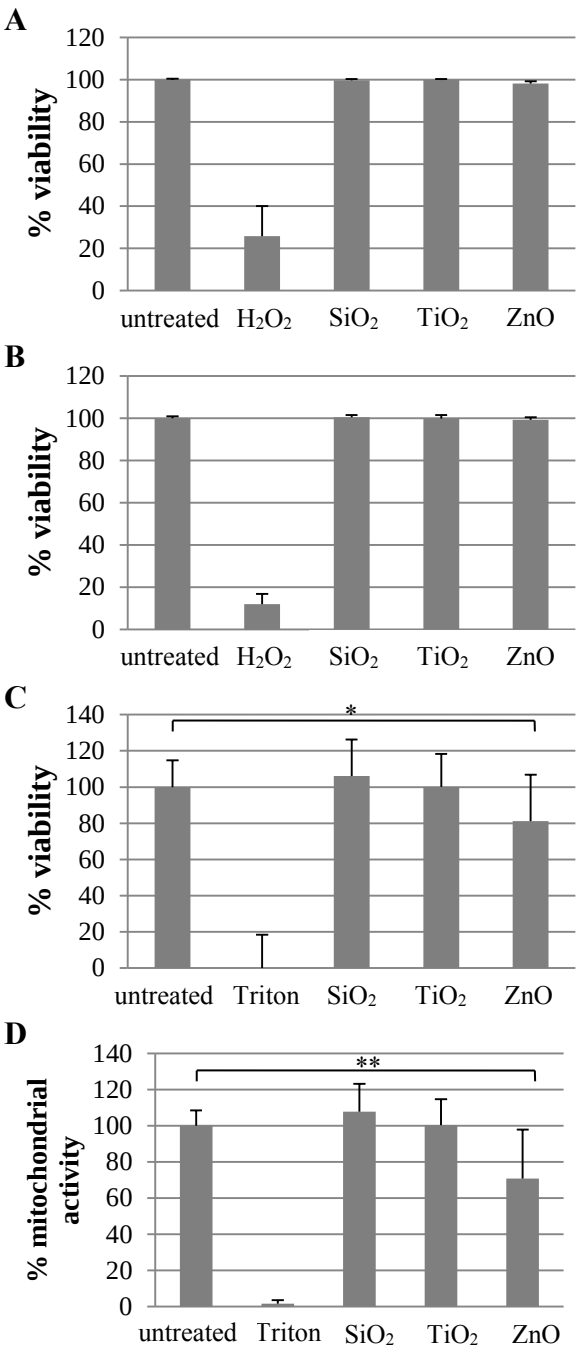

Figure 7. Results of cytotoxicity assays for C2BBe1 cells treated with nanoparticles in media for 24 hours. Hydrogen peroxide was used as a positive control to cause cell death in flow cytometric assays (A and B) while Triton X-100 served as a positive control for cell death in the colorimetric assays (C and D). A) Cells were stained with Sytox Red and analyzed by flow cytometry to monitor necrosis. B) Cells were stained with Annexin V and analyzed by flow cytometry to monitor apoptosis. C) LDH release into the supernatant was measured for membrane leakage. D) Reduction of MTT to formazan by mitochondrial enzymes was measured as an indicator of mitochondrial activity. Significance as compared to untreated controls in the LDH and MTT assays was measured by Student's *t*-test (* indicates $p<0.01$; ** indicates $p<0.0001$). Data are a compilation of five experiments, each containing three replicates.

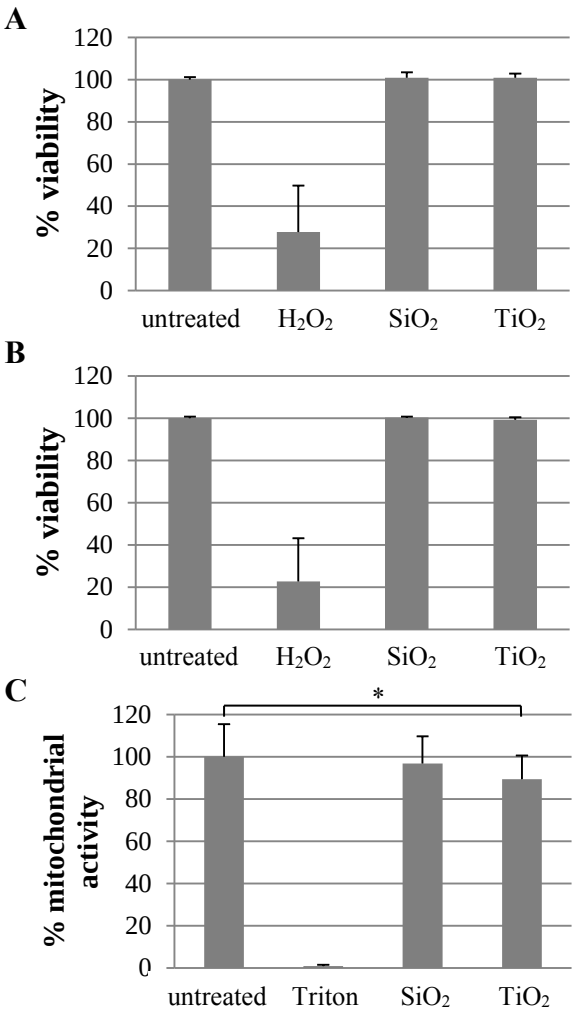

Figure 8. Cytotoxicity of C2BBe1 cells after treatment with simulated digestion media-treated SiO_2 and TiO_2 nanoparticles. Hydrogen peroxide was used as a positive control for cell death in flow cytometric assays (A and B) while Triton X-100 served as a positive control for cell death in the MTT assay (C). A) Cells were stained with Sytox Red and analyzed by flow cytometry to measure necrosis. Flow cytometry assay data are a compilation of three experiments, each containing three replicates. B) Cells were stained with Annexin V and analyzed by flow cytometry to measure apoptosis. C) Reduction of MTT to insoluble formazan was measured to indicate mitochondrial activity of these cells. Significance as compared to untreated controls in the MTT assay was measured by Student's *t*-test (* indicates $p<0.02$). MTT data are a compilation of four experiments, each containing three replicates.

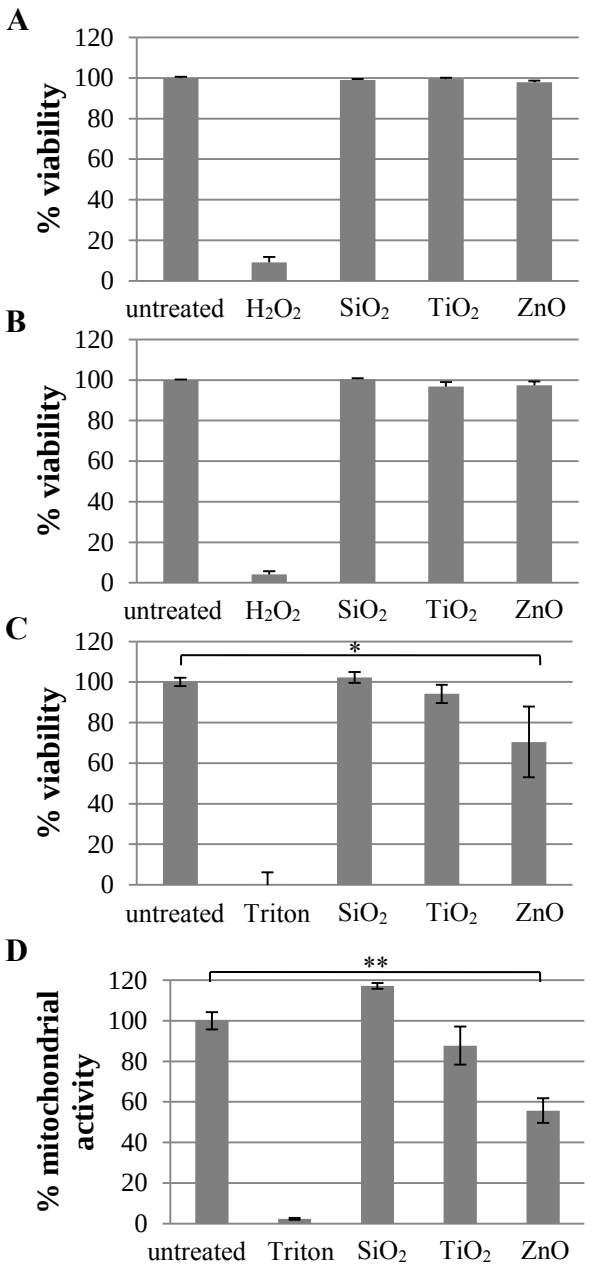

Figure 9. Toxicity assays were performed on C2BBe1 cells that had been repeatedly exposed to nanoparticles, approximately weekly. The assays were performed 24 hours after the most recent nanoparticle treatment. Representative data shown were obtained after 26 nanoparticle exposures. A) Cells were stained with Sytox Red and analyzed by flow cytometry to measure necrosis. B) Cells were stained with Annexin V and analyzed by flow cytometry to measure apoptosis. Flow cytometry assay experiment data (A and B) consists of 3 replicates for each treatment. C) LDH release by cells due to membrane damage was measured. D) Mitochondrial activity was assayed by reduction of MTT to formazan. LDH and MTT data consist of 4 replicates for each treatment. Significant differences in viability or mitochondrial activity as compared to untreated control was measured by Student's *t*-test (* indicates $p<0.01$; ** indicates $p<0.0001$) in LDH and MTT assays.

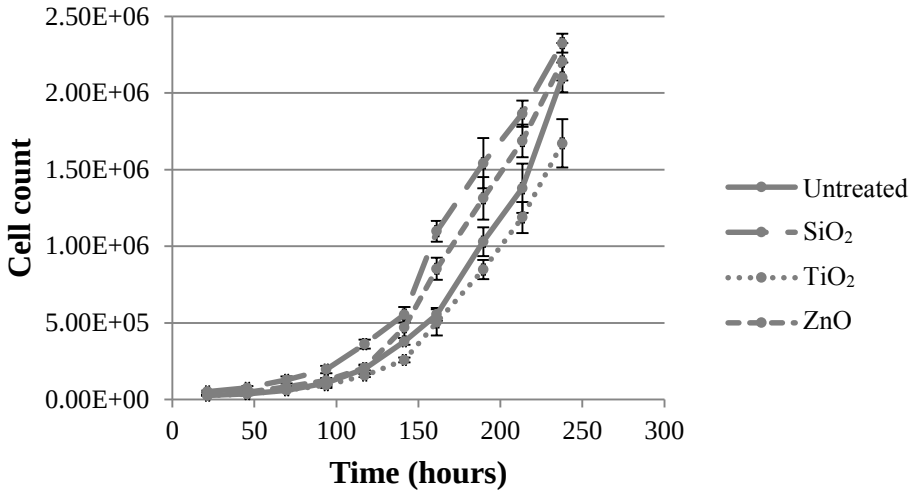

Figure 10. Growth curves after 11 nanoparticle exposure cycles. Growth was measured using cells that had undergone 11 cycles of repeated exposure to nanoparticles of SiO_2, TiO_2, or ZnO, along with untreated controls. Cells were plated at a starting concentration of 5×10^4 cells in 6-well tissue culture plates at time zero such that three replicate wells for each treatment could be counted daily for 10 days. This data is representative of growth curves performed after 7, 11, 16, and 29 nanoparticle exposures. Supporting Information shows the data for 29 exposures.

Supporting Information

Minimal intestinal epithelial cell toxicity in response to short- and long-term food-relevant inorganic nanoparticle exposure

Christie McCracken,[†] Andrew Zane,[‡] Deborah A. Knight,[†] Prabir K. Dutta,[,‡] and W. James Waldman,*[,†]*

[†]Department of Pathology, The Ohio State University College of Medicine, Columbus, Ohio 43210, United States

[‡]Department of Chemistry and Biochemistry, The Ohio State University, Columbus, Ohio 43210, United States

I. Procedure for DRIFTS analysis

Diffuse reflectance infrared Fourier transform spectroscopy (DRIFTS) was performed on particles which had undergone simulated digestion treatment. After the final digestion step, the particles were washed twice by centrifugation and replacement of supernatant with water. The digested particles were isolated by centrifugation and frozen with liquid nitrogen, then placed in a Millrock Bench Top Manifold Freeze Dryer (Millrock, Inc.) to preserve any potential protein coating. The digestion protocol was performed on another set of particles using water in place of digestive enzymes to use as reference. DRIFTS analysis was performed with a Spectrum 400 FTIR Imaging System (Perkin Elmer). Five hundred runs were performed in % Reflectance mode using an air background (mirror in the diffuse reflectance cell) for both the water and digested samples (50 mg); the samples were packed into the infrared cell without any dilution. Kubelka Munk analysis was performed on these samples using an in-house developed program using the air reference. The Kubelka Munk spectra of each water-exposed particle was subtracted from the spectra of each digested particle using Origin software, leaving only peaks related to the digestion enzymes and media (normalized relative to the 1260 cm^{-1} band observed in both TiO_2 and ZnO, and for SiO_2, the subtraction was done to maximize/symmetrize the band at 1300 cm^{-1}). An example of this for TiO_2 is shown in Figure S1.

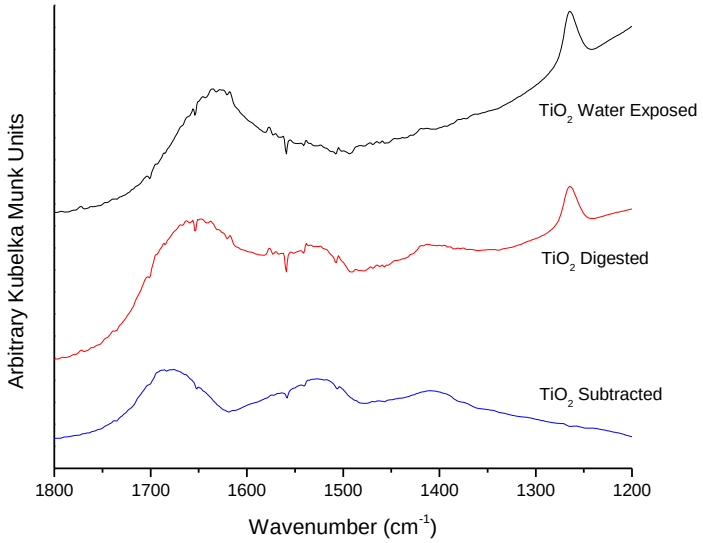

Figure S1. Example of DRIFTS subtraction process: TiO_2 exposed to water and freeze dried; TiO_2 treated with digestive solutions and freeze dried; and the subtraction of the water exposed spectra from the digested sample, leaving peaks related to the digestive enzymes.

II. Long-term nanoparticle exposure

Figure S2 shows two replicate growth curves performed after 29 nanoparticle exposures. While there is substantial inherent variability in proliferation rates among cultures treated identically (for example, compare proliferation curves of untreated controls shown in Figure S2 A and B), there is no consistent pattern of differences in proliferation rates between cells treated with the different nanoparticles that would suggest that any of these particles is more toxic than the others. Against the backdrop of this inherent variability in proliferation curves among replicate experiments, statistical analysis would not have provided meaningful information and hence was not performed.

A

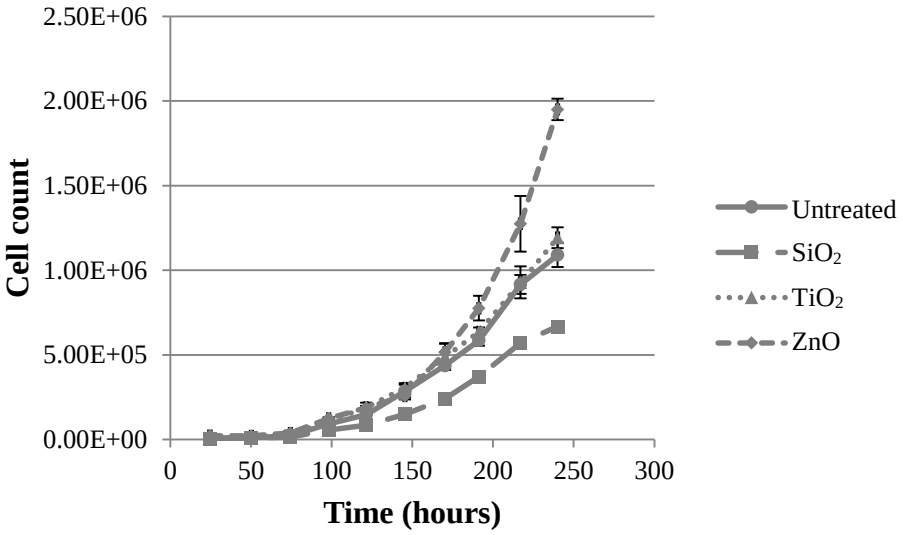

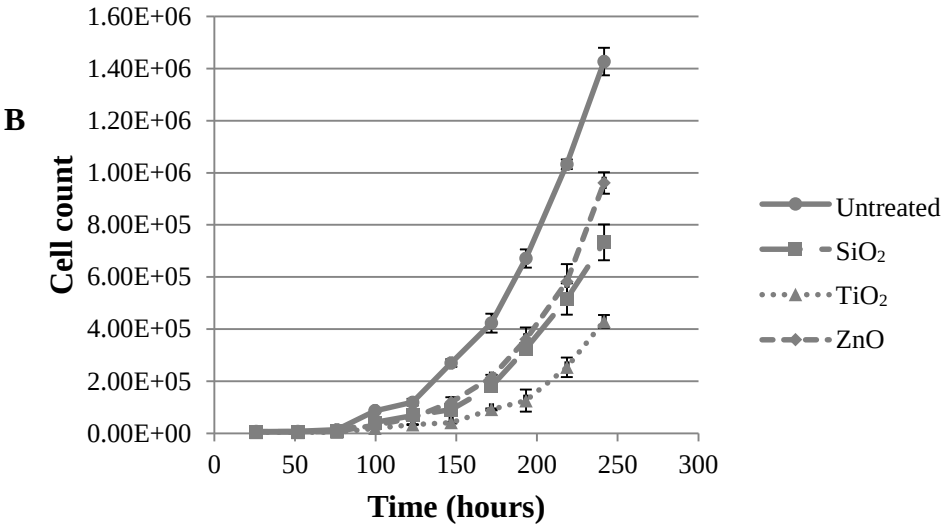

Figure S2. The growth curves shown above represent two replicate experiments conducted concurrently with cells that had undergone 29 nanoparticle exposures to SiO_2, TiO_2, or ZnO, as well as untreated controls cultured identically. Cells were plated at a concentration of 5×10^4 cells/well at time zero in 6-well tissue culture plates. This starting cell density allowed the three replicate wells for each treatment to be counted daily for 10 days without plateauing at confluence.